

Non-Solenoidal Formation of Spherical Torus by ECH/ECCD in LATE

H. Tanaka 1), T. Maekawa 1), M. Uchida 1), T. Yoshinaga 2), S. Nishi 1), Y. Kawazu 1),
K. Kurata 1), T. Takeuchi 1)

1) Graduate School of Energy Science, Kyoto University, Kyoto, Japan

2) National Institute for Fusion Science, Toki, Japan

e-mail contact of main author: h-tanaka@energy.kyoto-u.ac.jp

Abstract. Non-solenoidal formation of spherical torus by ECH/ECCD is performed in the LATE device. Plasma current is initiated and increased up to 20 kA with a 5 GHz, 190 kW, 70 ms microwave pulse, resulting in the formation of spherical tokamak. The ramp-up rate is ~ 300 kA/s, which is comparable to that by LHCD. The plasma current is carried by fast tail electrons. The tail electron energy increases as I_p increases, however, when $I_p > 15$ kA, tail velocity distribution becomes to be governed by the wave N_{\parallel} spectrum, not by particle confinement. Such tail electrons are driven along the field lines by EC heating toward higher velocity region far beyond the runaway velocity against the counter force from self induction, in much shorter time than the pitch angle diffusion time. Direct drive on tail electrons via EC absorption of high N_{\parallel} electron Bernstein waves should be working.

1. Introduction

In the conventional tokamaks such as ITER, the central solenoid (CS) is equipped to drive plasma current. At the start-up phase, inductive current generation by CS is used to ramp plasma current. But for the steady state operation in the burning phase, plasma current will be maintained non-inductively and CS will be almost useless. Recent conceptual designs of advanced tokamak reactors adopt removal of CS. They show many advantages. The core reactor structure becomes simple, its size becomes smaller and the construction cost is significantly reduced [1-3]. Especially, it is essential for spherical tokamaks because the central space is very limited. Various non-inductive current drive methods such as NBCD, LHCD and ECCD were successfully used to drive plasma current in MA level in the target plasmas produced inductively. But the scenario of non-inductive current start-up and ramping has not been established. Among the non-inductive current drive methods, ECH/ECCD is potentially attractive since the breakdown, current initiation and formation of closed flux surfaces can be realized by injection of microwave beams [4]. The equipment is just a small launcher which can be set at remote position from the plasma and is usable not only in the start-up phase but also in the burning phase for plasma control by local electron heating and current drive.

The LATE device has been exploring the feasibility of ECH/ECCD for non-solenoidal formation of spherical torus. Previously, the 3rd ECR layer was located near the center of the vacuum vessel and the plasma current I_p was saturated at 15 kA as the vertical field B_v was increased [5]. Recently, by increasing B_t as well as the microwave power so that the 2nd ECR layer locates near the vessel center, I_p increases without saturation and reaches 20 kA at a large ramp-up rate up to 300 kA/s. This fast ramp-up rate is comparable to that by LHCD [6-9]. In this paper, we report these recent experimental results. Firstly, we describe the experimental setup in the next section. Experimental results and discussions are presented in section 3. We summarize the results in Section 4.

2. Experimental Setup

The vacuum vessel of LATE is a stainless cylinder with diameter of 1 m and height of 1 m. The diameter of center post which cover the toroidal coil is 11.4 cm and there is no CS. After the previous Fusion Energy Conference, we made additional supports of return bars of the toroidal coil to hold the twisting electromagnetic force caused by the vertical magnetic field B_v . The operation at $B_t = 1$ kG at major radius $R = 25$ cm can be performed routinely under $B_v = 200$ G. The vertical field B_v is produced by 3 pairs of mirror-type coils whose currents are controlled by separate power supplies in pre-programmed waveforms respectively. There are two microwave sources at 5 GHz (≤ 200 kW, ≤ 0.07 sec) and 2.45 GHz (≤ 30 kW in total, ≤ 2 sec). The 5 GHz microwave pulse is injected through a circular waveguide antenna in the left-handed-circularly-polarized mode, with an angle of 15 degree to the radial direction on the mid-plane. This injection method aims for ECH/ECCD by electron Bernstein wave (EBW) converted via O-X-B process. The 2.45 GHz microwave pulse is injected in nearly the same way but in the linearly-polarized mode where the electric field vector is on the mid-plane. Main diagnostics are magnetic measurement by 17 flux loops, 70 GHz microwave interferometers for two different chord, 4 soft X-ray cameras with 80 chords on one poloidal cross section, a fast CCD camera for visible light plasma images and a spectrometer for visible light. A X-ray pulse height analysis (PHA) system with two Cd-Te detectors is also used to obtain photon energy spectra in energy range from 20 to 200 keV.

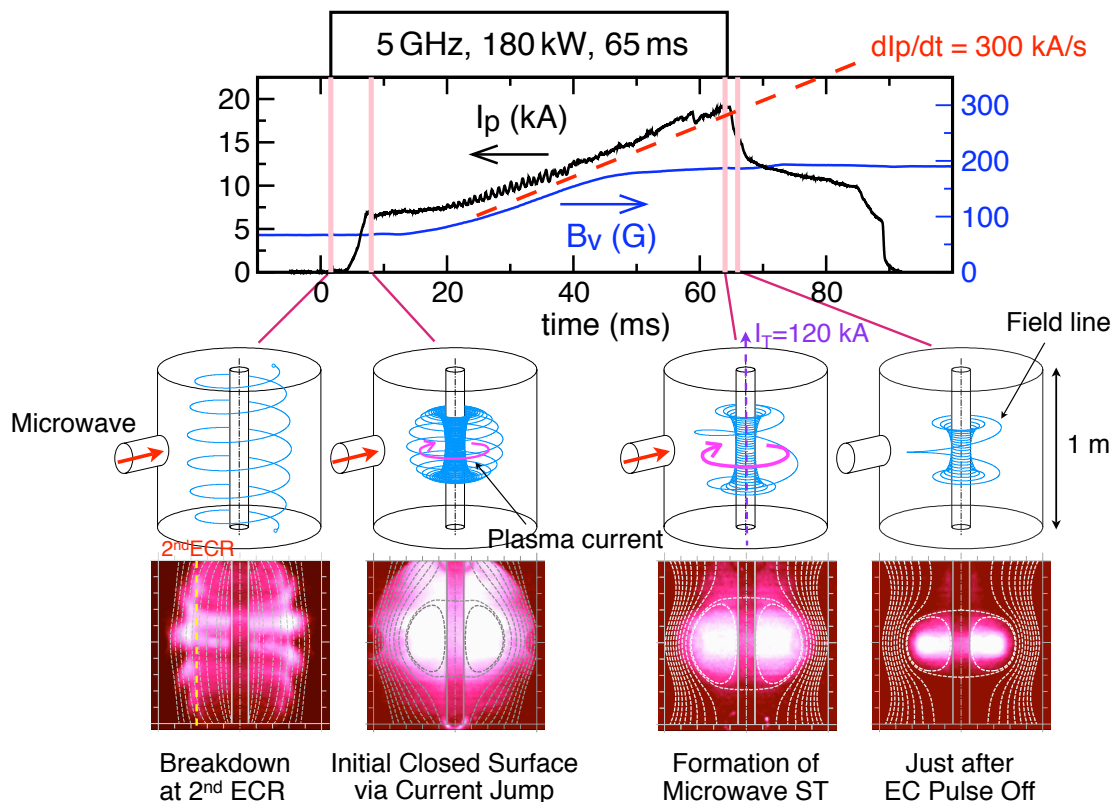


Fig. 1 Time evolution of plasma current, applied vertical field and field lines in a typical 5 GHz discharge. Visible-light plasma images are superimposed on the field lines.

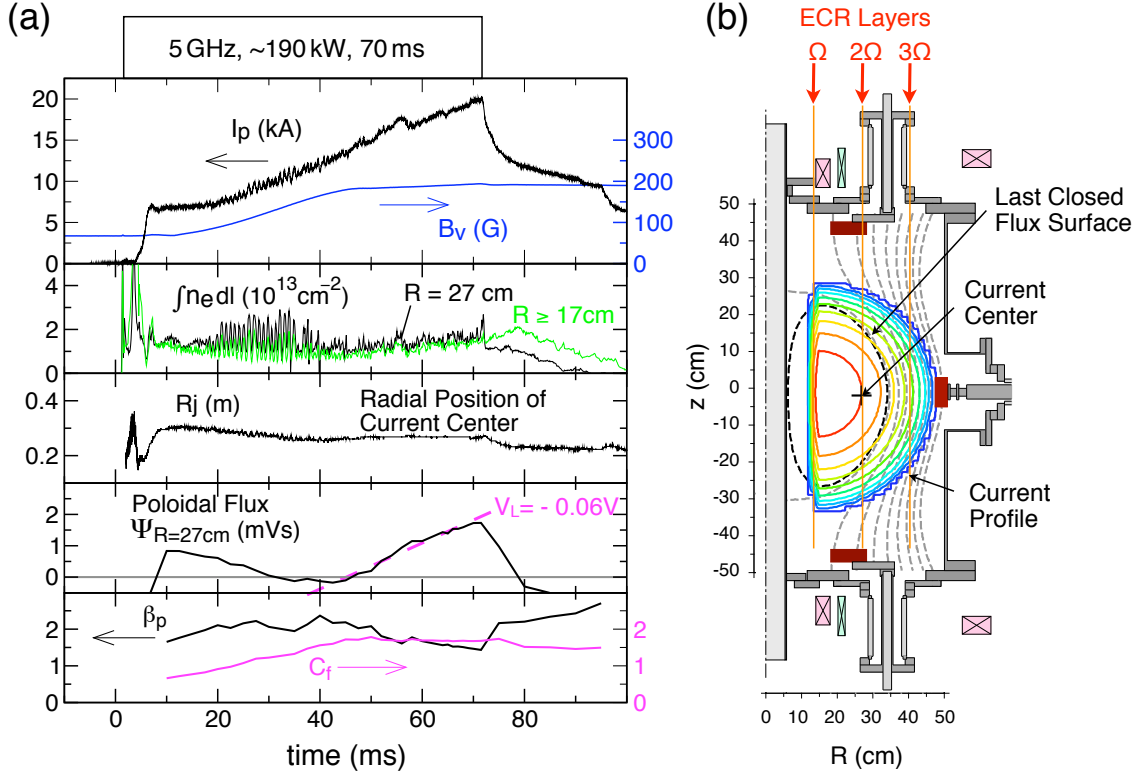


Fig. 2 (a) Time evolution of plasma current, applied vertical field, line-integrated electron density and quantities obtained from magnetic measurement. (b) Plasma current profile and flux surfaces at $I_p = 20$ kA.

3. Experimental Results and Discussions

Figure 1 shows the typical time evolution of the discharge with 5 GHz microwave. In this case, $B_t = 960$ G and the 2nd ECR layer locates at $R = 26.8$ cm. Applied vertical field is initially $B_v = 67$ G and the field line is like a vertical spring with a large pitch. The decay index of B_v is 0.13 and a weak magnetic mirror is formed. The filling pressure of hydrogen is $\sim 10^{-3}$ Pa. When the microwave power of 180 kW is injected, breakdown occurs along a field line at the 2nd ECR layer as shown in the visible-light image in Fig. 1. Plasma current I_p quickly increases up to 7 kA in 6.5 ms after the microwave injection and the initial closed flux surfaces are spontaneously formed under steady B_v . Then, as increasing B_v and decreasing the decay index, I_p ramps up at a rate of ~ 300 kA/s and reaches ~ 20 kA at the end of the 65 ms microwave pulse. The ratio of plasma current to the total toroidal coil current which flow in the center post is 1/6 and the field line on the last closed flux surface shows a spherical tokamak shape with an aspect ratio of 1.4 and an elongation of 1.8. The safety factor on the closed flux surface is about 30. In Fig. 2 (a), waveforms of line-integrated electron densities along two different chords and quantities obtained from magnetic measurement are shown. The line-averaged electron density is $\sim 4 \times 10^{11} \text{ cm}^{-3}$ and exceeds the plasma cutoff density at 5 GHz ($3.1 \times 10^{11} \text{ cm}^{-3}$). In Fig. 2 (b), plasma current profile and the last closed flux surfaces are plotted. The current profile as well as soft X-ray emission profile encompass the 2nd and the 3rd ECR layers. These facts suggest that EBW heat the plasma and drive I_p . The poloidal beta β_p is large (1.4 \sim 2) during the discharge and is essentially due to the current-carrying tail electrons. Contribution of bulk electrons is only ~ 0.05 as estimated from the bulk density and temperature $T_e \sim 60$ eV. Evidences that the plasma current is carried by the fast tail electrons

are as follows. Firstly, the average parallel electron drift speed $\langle v_{\parallel} \rangle = I_p / en_e S$ is large ($\sim 3 \times 10^6$ m/s when $I_p = 20$ kA, $n_e = 4 \times 10^{11}$ cm $^{-3}$ and poloidal cross section $S = 0.1$ m 2) and comparable to the electron thermal speed $v_{th} = (2T_e/m_e)^{1/2} = 4.6 \times 10^6$ m/s for $T_e = 60$ eV). Secondly, the average electron energy $\langle W \rangle = \mu_0 I_p^2 \beta p / 8\pi S n_e$ estimated from $\beta p = 8\pi S \langle p \rangle / \mu_0 I_p^2$ is high (~ 4.7 keV when $I_p = 20$ kA, $n_e = 4 \times 10^{11}$ cm $^{-3}$, $S = 0.1$ m 2 and $\beta p = 1.5$). Thirdly, current profile is shifted outward from the last closed flux surface (Fig. 2 (b)). In the axisymmetric system, canonical angular momentum is conserved as $P_{\varphi} = m_e \gamma R v_{\varphi} - e\Psi / 2\pi = \text{const}$. Here, m_e is electron's mass, γ is relativistic factor, e is elementary charge and Ψ is poloidal flux. When the electron energy is low and I_p is large, the second term in the right-hand side is dominant and the electron drifts on the constant Ψ surface. On the other hand, when the electron energy is high and I_p is small, the first term is not negligible and the electron orbit shifts from the flux surface. The orbits of the current-carrying tail electrons shift outward, which corresponds to the outward-shifted current profile.

Direct detection of such current-carrying tail electrons is done by X-ray PHA of bremsstrahlung emission. Figure 3 (a) shows the schematic view of the X-ray PHA system. We set two Cd-Te detectors such that both line-of-sights are tangent to the circle with major radius $R = 25$ cm on the mid-plane near where the current center is positioned. The lead collimation systems are the same and the viewing solid angles are the same. The "Forward" detector detects X-rays emitted by the current-carrying tail electrons in their drift direction and the "Backward" detector detects X-rays emitted by them in their anti-drift direction. When the electron energy

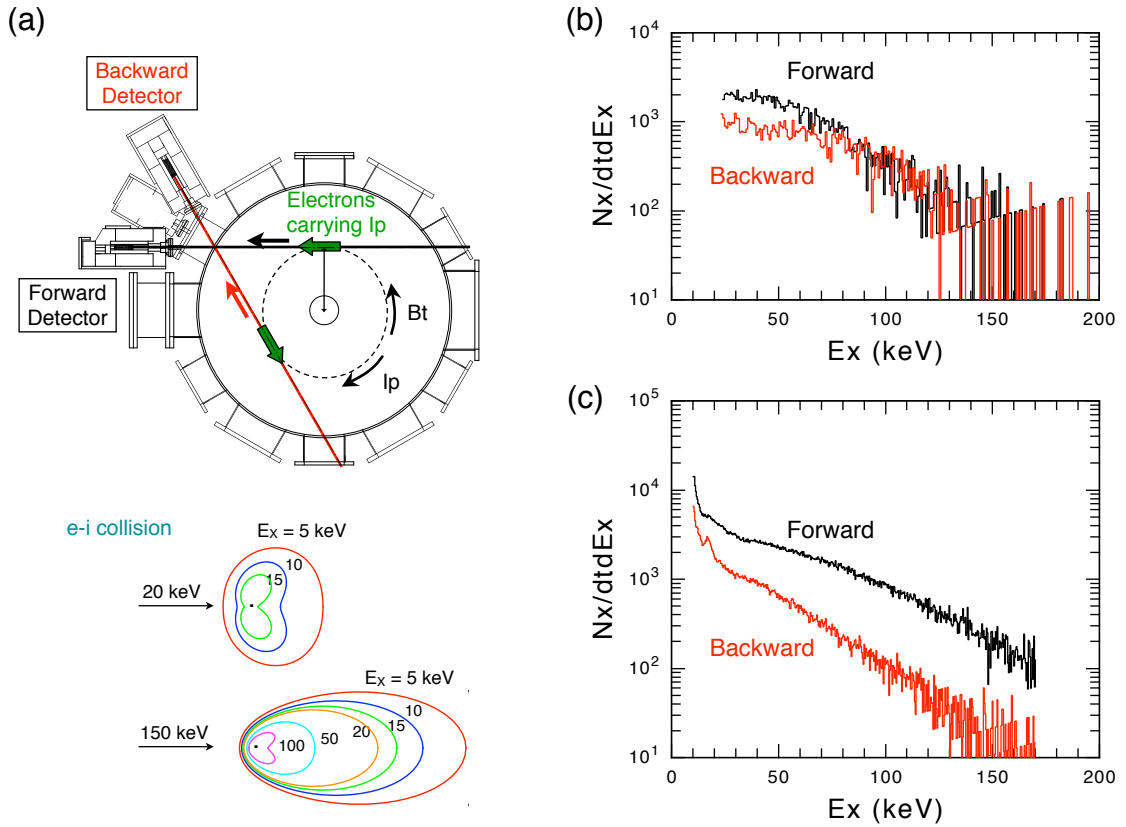


Fig. 3 (a) Schematic view of X-ray pulse-height-analysis system and polar plot of X-ray intensity of bremsstrahlung emission in the case of $e-i$ collision. X-ray energy spectra of forward (black) and backward (red) emissions in (b) 5 GHz discharges at $I_p = 8.5 - 11.5$ kA and (c) 2.45 GHz discharges at $I_p = 5.9$ kA.

is high, the radiation lobes of bremsstrahlung emission strongly shift forwardly along the electron drift direction by the relativistic effect as shown in Fig. 3 (a). Therefore, intensity ratio of both detectors indicates the anisotropy of tail velocity distribution along the magnetic field. The X-ray energy spectra shown in Fig. 3 (b) are obtained in the 5 GHz discharges with 10 ms gate duration. During this period, plasma current increases from 8.5 to 11.5 kA. Forward intensity is about two times greater than backward one in the photon energy range up to ~ 70 keV. The X-ray energy spectra shown in Fig. 3 (c) are obtained in the 2.45 GHz discharges with 200 ms gate duration by taking advantage of relatively long pulse length. During this period, plasma current is constant at 5.9 kA. The intensity ratio of forward one to backward one is ~ 10 for photon energy $E_x \sim 150$ keV, which implies a uni-directional fast electron tail drifting in the current-carrying direction. Time evolution of X-ray energy spectra shows that the X-ray intensity and energy range as well as the ratio of forward intensity to backward one also increase as I_p increases, suggesting that the anisotropic velocity distribution of fast tail electrons is generated and enhanced during current ramp-up.

The time evolution of tail electron energy is also estimated from magnetic measurement. If the tail electron velocity distribution function $f(\mathbf{v})$ is spatially uniform, βp is written (neglecting the contribution of bulk electrons) by $\beta p = 8\pi S \langle p \rangle / \mu_0 I_p^2 = 8\pi \langle p \rangle / \mu_0 I_p J = C_f I_A / I_p$, where $I_A = 4\pi m_e c / \mu_0 e \approx 17$ kA and

$$C_f = \frac{2 \int \left(\frac{1}{2} \gamma v_{\parallel}^2 + \frac{1}{4} \gamma v_{\perp}^2 \right) f(\vec{v}) d^3 \vec{v}}{c \int v_{\parallel} f(\vec{v}) d^3 \vec{v}}$$

is a dimensionless factor which is a measure of the tail momentum range [10, 11]. (For example, when the tail pressure can be written as $p \sim n m_e \gamma v^2 / 2$ for the typical velocity v and the current density as $J = I_p / S \sim n e v$. Then, the factor $C_f = I_p \beta p / I_A = (2e / m_e c) (\langle p \rangle / J) \sim \gamma v / c$, which coincides with the normalized momentum.) Therefore average tail energy can be estimated by $\langle \varepsilon_f \rangle = m_e c^2 ((1 + C_f^2)^{1/2} - 1)$ where $C_f = I_p \beta p / I_A$ is obtained from magnetic measurement. In the 2.45 GHz discharges with I_p up to 5.9 kA as in Fig. 3 (c), it is confirmed that $\langle \varepsilon_f \rangle$ increases from 10 to 75 keV as I_p increases and it is consistent with the time evolution of X-ray energy spectra.

To investigate the experimental result that tail electron energy increases as I_p increases, we calculated electron orbits in the steady magnetic field as obtained from magnetic measurement. Figure 4 (a) shows that passing electrons who drift in the current-carrying direction with energy more than ~ 180 keV hit against the outer wall or limiter at $R = 47$ cm (see Fig. 2 (b)) when $I_p = 5.9$ kA (as in Fig. 3 (c)). Figure 4 (b) shows that passing electrons who drift in the current-carrying direction with energy more than ~ 550 keV hit against the outer wall or limiter at $R = 47$ cm when $I_p = 12.5$ kA. Figure 4 (c) shows that when $I_p = 20$ kA (as in Fig. 2 (b)), passing electrons who drift in the current-carrying direction with energy of 1 MeV can go round without hitting wall nor limiter. These calculation show that cutoff energy of passing electrons increases with I_p . Then increase of tail electron energy may be due to improvement of high energy particle confinement.

In the case of the 5 GHz discharge as shown in Fig. 2, C_f increases initially as I_p increases, then it becomes steady when $I_p > 15$ kA $\sim I_A$. This means that while the tail momentum range is limited by the orbit loss due to the outward shift of electron orbit from the flux surfaces, the

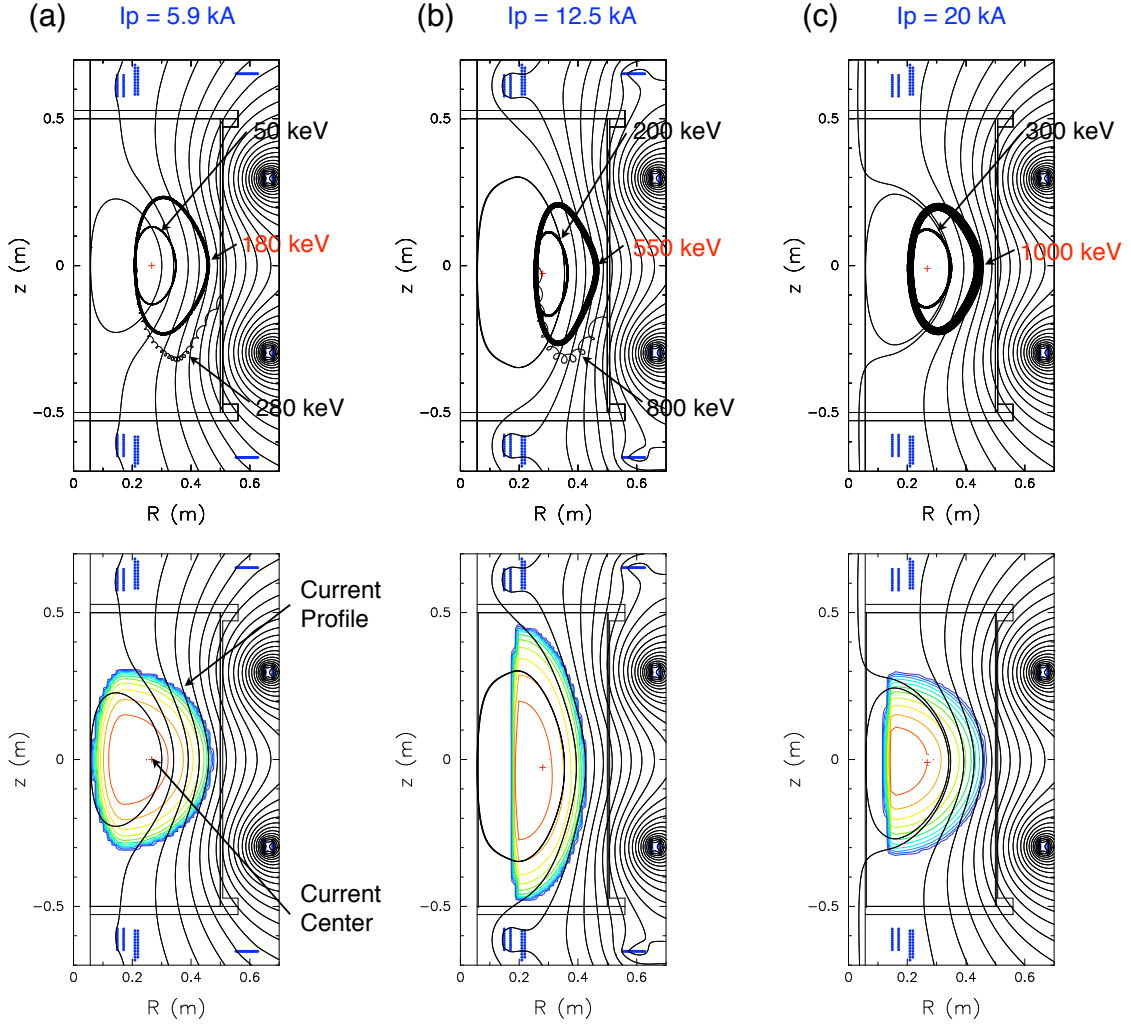


Fig. 4 Orbits of passing electrons (upper) calculated in the observed magnetic field and current profile (lower) for (a) $I_p = 5.9$ kA in 2.45 GHz discharge, (b) $I_p = 12.5$ kA and (c) $I_p = 20$ kA in 5 GHz discharge. Field lines are superimposed.

shift becomes small at $I_p > 15$ kA and the tail velocity distribution is rather determined by the wave N_{\parallel} spectrum. This is a new regime and not obtained previously.

As shown in Fig. 2 (a), poloidal flux at $R = 27$ cm (near the current center position) increases during fast ramp-up phase $t > 45$ ms. This variation of poloidal flux corresponds to a negative loop voltage of $V_L = -0.06$ V. It is remarkable that I_p increases against the reverse voltage due to the self-induction. The tail energy range estimated from C_f at $I_p = 20$ kA is as large as ~ 500 keV, which exceeds the runaway critical energy ~ 2 keV for the reverse voltage of $V_L = -0.06$ V. The production of such high energy tail at the energy range far beyond the critical energy where the reverse electric force is much larger than the collisional friction force is essential for efficient current ramp-up. This was already realized for LHCD but not for ECCD so far.

As for the mechanism of creation of such anisotropic tail velocity distribution along the magnetic field, it is usually thought that EC resonant electrons are heated nearly perpendicularly to the magnetic field and subsequent pitch angle scattering to the forward confinement region in the velocity space may build up the anisotropic tail distribution. However, the current

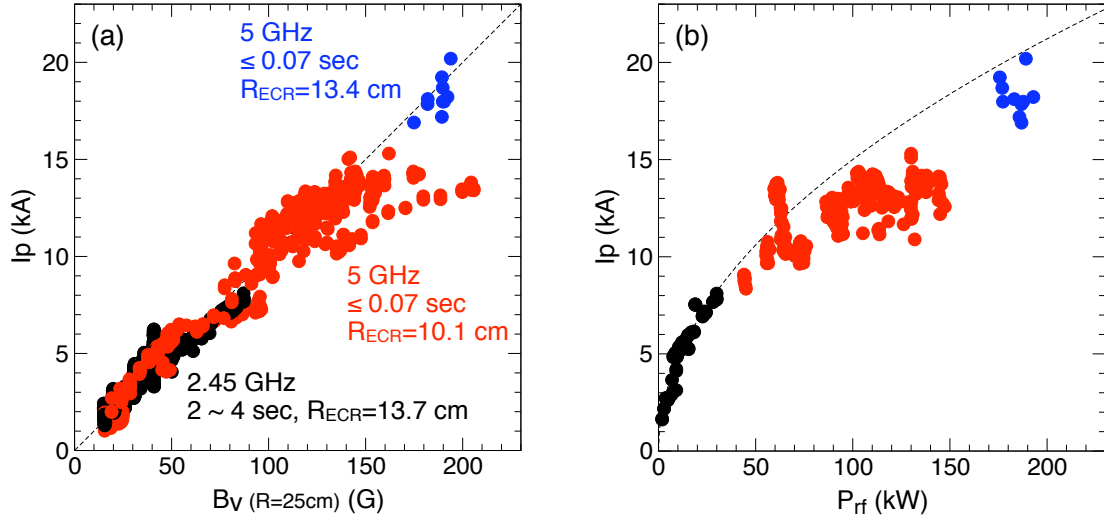


Fig. 5 Maximum plasma current as a function of (a) applied vertical field at $R = 25$ cm, and (b) injected net microwave power.

ramp-up time (~ 50 ms) is two orders of magnitude shorter than the 90 degree scattering time for fast tail electrons (with energy ~ 200 keV) in the present discharges and this mechanism may not work. Moreover, measurement of heat load on limiters shows that 20 - 50 % of P_{rf} is lost to limiters due to fast electron direct loss. Then, generation of high energy tail far beyond the critical energy under large spatial loss strongly suggest the presence of some direct forward force on the tail electrons. It may be realized by EC absorption of high $N_{||}$ EBW because EC resonant electrons gain velocity at the ratio $\delta v_{||}/\delta v_{\perp} = N_{||}(v_{\perp}/c)/(l\Omega/\omega)$, where $N_{||}$ is the parallel refractive index, Ω is the EC frequency, l is the harmonic number and ω is the wave frequency.

Maximum plasma currents obtained in various discharge conditions are plotted as a function of B_v and injected net microwave power P_{rf} in Fig. 5. Blue closed circles show data obtained recently and red ones show previous data. Previous data were obtained under lower B_t such that the 3rd ECR layer was located near the center of the vacuum vessel. The plasma current I_p was saturated at ~ 15 kA as the vertical field B_v was increased. By increasing B_t and positioning the 2nd ECR layer near the center of the vacuum vessel, I_p becomes proportional again to B_v . This means that a good MHD equilibrium with a large last closed flux surface is achieved. It may be due to the better coupling of mode-converted EBW to fast tail electrons which carry I_p . The maximum plasma current is proportional to a square root of P_{rf} within present discharge parameters. This result means that the stored magnetic energy is proportional to P_{rf} and conversion efficiency from microwave energy to magnetic energy is constant in the power range $P_{rf} \leq 200$ kW.

4. Summary

Plasma current is started and ramped up to 20 kA without CS by injecting a 5 GHz, 190 kW, 70 ms microwave pulse, resulting in the formation of spherical tokamak. The current ramp up rate is ~ 300 kA/s, which is comparable to that in the LHCD case. The line-averaged electron density exceeds the plasma cutoff density and the current center position locates near the 2nd ECR layer, suggesting ECH/ECCD by EBW. Fast electron tail that carries the plasma current

is generated and developed toward higher velocity range as I_p increases. In the final stage of larger current near I_A , however, tail velocity distribution becomes to be governed by the wave $N_{//}$ spectrum, not by particle confinement. Such tail electrons are driven along the field lines by EC heating toward higher velocity region far beyond the runaway velocity against the counter force from self induction, in much shorter time than the pitch angle diffusion time. Direct drive on tail electrons via EC absorption of high $N_{//}$ EB waves should be working.

References

- [1] PENG, Y.-K.M., et al., Proc. 20th Fusion Energy Conf., IAEA-CN-116/FT/3-1Rb, 2004.
- [2] NISHIO, S., et al., Proc. 20th Fusion Energy Conf., IAEA-CN-116/FT/P7-35, 2004.
- [3] TOBITA, K., et al., Proc. 21st Fusion Energy Conf., IAEA-CN-149/FT/P5-21, 2006.
- [4] YOSHINAGA, T., et al., Phys. Rev. Lett., 96 (2006) 125005.
- [5] TANAKA, H., et al., Proc. of 21st Fusion Energy Conf., IAEA-CN-149/EX/P6-6, 2006.
- [6] KUBO, S., et al., Phys. Rev. Lett., 50 (1983) 1994.
- [7] JOBES, F., et al., Phys. Rev. Lett., 52 (1984) 1005.
- [8] TOI, K., et al., Phys. Rev. Lett., 52 (1984) 2144.
- [9] OGURA, K., et al., Nucl. Fusion, 30 (1990) 611.
- [10] SHAFRANOV, V. D., Plasma Phys., 13 (1971) 757.
- [11] MONDELLI, A. and OTT, E., Phys. Fluids, 17 (1974) 1017.